

Thermodynamics of two-colour QCD and the Nambu Jona-Lasinio model ^{*}

Claudia Ratti ^a and Wolfram Weise ^{a,b}

^a Physik-Department, Technische Universität München, D-85747 Garching, Germany

^b ECT*, I-38050 Villazzano (Trento), Italy

July 29, 2021

Abstract

We investigate two-flavour and two-colour QCD at finite temperature and chemical potential in comparison with a corresponding Nambu and Jona-Lasinio model. By minimizing the thermodynamic potential of the system, we confirm that a second order phase transition occurs at a value of the chemical potential equal to half the mass of the chiral Goldstone mode. For chemical potentials beyond this value the scalar diquarks undergo Bose condensation and the diquark condensate is nonzero. We evaluate the behaviour of the chiral condensate, the diquark condensate, the baryon charge density and the masses of scalar diquark, antidiquark and pion, as functions of the chemical potential. Very good agreement is found with lattice QCD ($N_c = 2$) results. We also compare with a model based on leading-order chiral effective field theory.

^{*}Work supported in part by INFN and BMBF

1 Introduction

The phase structure of QCD has been subject of intense investigations in recent years. Precise numerical data have become available concerning QCD thermodynamics at high temperature via large-scale computer simulations on the lattice (for a review see [1]). The study of full QCD at finite baryon density is still a formidable challenge, due to the limitations of standard Monte Carlo simulations when applied to systems at finite chemical potential (for recent results see [2, 3]). Present developments are aimed at improved strategies [4] to deal with the fact that the determinant of the Euclidean Dirac operator becomes complex at finite chemical potential.

An interesting perspective of finite-density QCD is the emergence of colour superconductivity (CSC). This was revealed first by calculations based on one-gluon exchange: Barrois, Bailin and Love [5, 6] and later Iwasaki and Iwado [7] pointed out that the induced attractive force near the Fermi surface creates quark Cooper pairs resulting in CSC in the case of QCD at low temperature and high density. In the late nineties, using an instanton model of the effective interaction, Alford, Rajagopal and Wilczek [8, 9] and Rapp, Schäfer, Shuryak and Velkovsky [10] argued that the energy gap is expected to be of the order of 100 MeV.

No first principle computations exist at this moment concerning the phenomenon of colour superconductivity in full $N_c = 3$ QCD. One response to this situation has been to start from simpler QCD-like theories with additional antiunitary symmetries that guarantee the Fermion determinant to be real at non-zero chemical potential and therefore allow the study of such theories on the lattice. Examples of such explorations include QCD with two colours and fundamental quarks and QCD with an arbitrary number of colours and adjoint quarks [11]. The physics of both these theories is quite different from full three-colour QCD. Nevertheless these differences are easily understood and classified. Knowledge of the critical conditions for phase transitions in these schematic cases may offer qualitative clues about critical phenomena encountered in three colour QCD, such as diquark condensation.

In two-colour QCD, diquarks can form colour singlets which are the baryons of the theory. The lightest baryons and the lightest quark-antiquark excitations (pions) have a common mass, m_π , and this spectrum determines the properties of the ground state for small chemical potentials. General arguments [12] predict a phase transition from the vacuum to a state with finite baryon density at a critical chemical potential μ_c , which is the lowest energy per quark that can be realized by an excited state of the system. This state is populated by light diquarks, and one expects $\mu_c = m_\pi/2$. The Bose-Einstein condensation of diquarks, with nonzero baryon number, can be interpreted as baryon charge superconductivity.

The (T, μ) phase diagram of QCD with two colours has been studied by Dagotto *et al.* using a mean-field model of the lattice action [13, 14]. The smallness of μ_c has been exploited to study the zero temperature phase transition using a chiral

effective Lagrangian extended to the flavour symmetry $SU(2N_f)$ [11, 15–18]. Other approaches to two-colour QCD have also been explored, based for example on a random matrix model [19, 20] and on the renormalization group [21]. Several of these model calculations have been verified by lattice simulations [22–41].

In the present paper we investigate the relationship between $N_c = 2$ QCD and a corresponding Nambu and Jona-Lasinio (NJL) model [42–46] in which gluonic degrees of freedom are “integrated out” and replaced by a local four-point interaction of quark colour currents. This amounts to effectively replacing the local colour gauge symmetry by a global one, with the assumption that coloured (gluonic) excitations are far removed from the low-energy spectrum and hence “frozen”. Similar models have already been used to study the QCD colour superconductivity phase with two [47–51] and three flavours [52–54] (for a recent review see [55]). The specific aim of this work is to test the effectiveness of the NJL model, with its dynamically generated quasiparticles, in reproducing the thermodynamics of two-colour QCD, and to compare our results quantitatively with those obtained from recent lattice computations. We study the behaviour of the chiral and diquark condensates, and of the baryon density, as functions of temperature and chemical potential, both in the chiral limit and for finite values of the current quark masses. We investigate, again for both zero and finite quark masses, the two-colour QCD phase diagram in the T - μ plane. As further applications we evaluate the pion, diquark and antidiquark masses, as functions of the chemical potential. We compare our results to lattice data and also to the predictions from chiral effective field theory.

2 Two colour NJL model

Consider as a starting point the Lagrangian

$$\mathcal{L} = \bar{\psi}(x) (i\gamma^\mu \partial_\mu - \mathbf{m}_0) \psi(x) - G_c \sum_{a=1}^3 J_\mu^a(x) J_a^\mu(x), \quad (1)$$

with a four point interaction that represents the local coupling between colour currents $J_\mu^a = \bar{\psi} \gamma_\mu t^a \psi$ involving the quark fields ψ and the $SU(2)_{colour}$ generators t_a with $tr(t^a t^b) = 2\delta_{ab}$. Here G_c is an effective coupling strength of dimension $(\text{length})^2$ and \mathbf{m}_0 is the diagonal current quark mass matrix.

In this paper we restrict ourselves to the case of two quark flavours ($N_f = 2$). In this case there are only two order parameters, the quark condensate $\langle \bar{\psi} \psi \rangle$ and the scalar diquark condensate, symbolically denoted by $\langle \psi \psi \rangle$. It is convenient to rewrite the interaction between quarks, by Fierz transformation, in terms of the colour singlet pseudoscalar/scalar quark-antiquark and scalar diquark channels. The resulting Lagrangian reads

$$\mathcal{L}_{NJL} = \bar{\psi} (i\gamma^\mu \partial_\mu - \mathbf{m}_0) \psi + \mathcal{L}_{q\bar{q}} + \mathcal{L}_{qq} + (\text{colour triplet terms}), \quad (2)$$

$$\begin{aligned}\mathcal{L}_{q\bar{q}} &= \frac{G}{2} \left[(\bar{\psi}\psi)^2 + (\bar{\psi}i\gamma_5\vec{\tau}\psi)^2 \right], \\ \mathcal{L}_{qq} &= \frac{H}{2} (\bar{\psi}i\gamma_5\tau_2t_2C\bar{\psi}^T) (\psi^TCi\gamma_5\tau_2t_2\psi)\end{aligned}$$

where G and H are constants which describe quark-antiquark and quark-quark interactions, respectively, t_a are Pauli matrices in colour space and τ_i are Pauli matrices in flavour (isospin) space. We have introduced the charge conjugation operator for fermions:

$$C = i\gamma_0\gamma_2. \quad (3)$$

The coupling constants G and H in the Lagrangian (2) are fixed by Fierz transforming the colour-current interaction in (1) to obtain

$$G = H = \frac{3}{2}G_c \quad (4)$$

(see the Appendix for details).

As mentioned, the local $SU(N_c = 2)$ gauge symmetry is replaced by global $SU(2)_{colour}$ in this model. In the chiral limit, the Lagrangian (2) is invariant under an enlarged flavour symmetry $SU(N_f) \times SU(N_f) \times U(1) \rightarrow SU(2N_f)$, which connects quarks and antiquarks: the so-called Pauli-Gürsey symmetry, a characteristic feature of two-colour QCD. This symmetry relates pions and scalar diquarks. It is a natural ingredient of the “equivalent” NJL model, with eq. (4) relating the coupling constants of the model Lagrangian.

Starting from the Lagrangian (2) and using standard bosonization techniques, we introduce the auxiliary scalar (σ), pseudoscalar triplet¹ ($\vec{\pi}$) and diquark (Δ, Δ^*) fields, thus obtaining the following equivalent Lagrangian in the colour singlet sector:

$$\begin{aligned}\tilde{\mathcal{L}} &= \bar{\psi} (i\gamma^\mu\partial_\mu - \mathbf{m}_0 + \sigma + i\gamma_5\vec{\tau} \cdot \vec{\pi}) \psi - \frac{1}{2}\Delta^*\psi^TC\gamma_5\tau_2t_2\psi \\ &+ \frac{1}{2}\Delta\bar{\psi}\gamma_5\tau_2t_2C\bar{\psi}^T - \frac{\sigma^2 + \vec{\pi}^2}{2G} - \frac{|\Delta|^2}{2H}.\end{aligned} \quad (5)$$

It is useful to represent the quark fields by a bispinor defined in the following way:

$$q(x) = \frac{1}{\sqrt{2}} \begin{pmatrix} \psi(x) \\ C\bar{\psi}^T(x) \end{pmatrix}. \quad (6)$$

Furthermore, we introduce the matrix propagator

$$S^{-1}(p) = \begin{pmatrix} \not{p} - \hat{M} & \Delta\gamma_5\tau_2t_2 \\ -\Delta^*\gamma_5\tau_2t_2 & \not{p} - \hat{M} \end{pmatrix} \quad (7)$$

¹Isovectors such as the pion field are denoted by $\vec{\pi}$.

(the inverse of the so-called Nambu-Gorkov propagator) where we have defined

$$\hat{M} = (m_0 - \sigma)\mathbf{1} - i\gamma_5 \vec{\tau} \cdot \vec{\pi}; \quad (8)$$

here $\mathbf{1} = \mathbf{1}_c \cdot \mathbf{1}_f \cdot \mathbf{1}_D$ is the unit matrix in colour, flavour and Dirac indices. We consider the flavour-symmetric case with $m_u = m_d \equiv m_0$. Integrating over $q(x)$ and $\bar{q}(x)$ we obtain the effective Lagrangian in terms of the auxiliary field variables $\sigma, \vec{\pi}, \Delta$ and Δ^* . It can be written as:

$$\mathcal{L}_{eff} = -\frac{\sigma^2 + \vec{\pi}^2}{2G} - \frac{|\Delta|^2}{2H} - i \int \frac{d^4p}{(2\pi^4)} \frac{1}{2} \text{Tr} \ln (S^{-1}(p)). \quad (9)$$

The trace in this expression is taken over flavour, colour and Dirac indices, and the factor $\frac{1}{2}$ compensates for double-counting in the q and \bar{q} fields.

Solving the field equations for $\sigma, \vec{\pi}, \Delta$ and Δ^* and working in the mean field approximation², we can evaluate their vacuum expectation values. The mean field value $\langle \vec{\pi} \rangle$ of the pseudoscalar isotriplet field is always equal to zero. The σ field has a non-vanishing vacuum expectation value as a consequence of spontaneous chiral symmetry breaking, while the diquark fields Δ and Δ^* are expected to have nonzero mean values only in dense matter. An interesting limiting situation is encountered when $m_0 = 0$ (chiral limit) together with $\mu = 0$. In this limit the extended $SU(2N_f)$ symmetry with $N_f = 2$ (and $G = H$) implies that the thermodynamic potential depends only on $R^2 = \sigma^2 + |\Delta|^2$ so that there is a degeneracy along the circle with constant radius R . This case will be further discussed in section 5.

After solving the field equation for σ , we can work in terms of the effective quark mass m which is related to $\langle \sigma \rangle$ through the self-consistent gap equation

$$m = m_0 - \langle \sigma \rangle = m_0 - G \langle \bar{\psi} \psi \rangle. \quad (10)$$

Note that $\langle \sigma \rangle = G \langle \bar{\psi} \psi \rangle$ is negative in our representation, and $\langle \bar{\psi} \psi \rangle = \langle \bar{\psi}_u \psi_u + \bar{\psi}_d \psi_d \rangle$ with $\langle \bar{\psi}_u \psi_u \rangle = \langle \bar{\psi}_d \psi_d \rangle$.

3 Parameter fixing

The three parameters of the model are the ‘‘bare’’ quark mass m_0 , a loop-momentum cutoff Λ and the coupling strength $G = H$. Even if we are considering the $N_c = 2$ NJL model, we choose to reproduce the known chiral physics in the hadronic sector. This is reasonable since, in colour singlet channels, N_c enters only parametrically in the relevant physical constants and observables. For this reason, we fix those parameters through the constraints imposed by the pion decay constant and the chiral (quark) condensate:

²In the mean field approximation the fields are replaced by their expectation values for which we will later on continue using the notation σ and Δ for simplicity and convenience.

Λ [GeV]	$G = H[\text{GeV}^{-2}]$	$m_0[\text{MeV}]$	$m[\text{MeV}]$	$ \langle\bar{\psi}_u\psi_u\rangle ^{1/3}[\text{MeV}]$	$f_\pi[\text{MeV}]$	$m_\pi[\text{MeV}]$
0.78	10.3	4.5	361	259	89.6	139.3

Table 1: Parameter set used in this work, and the corresponding physical quantities.

- The pion decay constant f_π is evaluated in the NJL model through the following relation:

$$f_\pi^2 = 4m^2 I_\Lambda^{(1)}(m) \quad \text{where} \quad I_\Lambda^{(1)}(m) = -iN_c \int \frac{d^4p}{(2\pi)^4} \frac{\theta(\Lambda^2 - \vec{p}^2)}{(p^2 - m^2 + i\epsilon)^2}. \quad (11)$$

The empirical value is $f_\pi = 92.4$ MeV.

- The quark condensate becomes

$$\langle\bar{\psi}_u\psi_u\rangle = -4mI_\Lambda^{(0)}(m) \quad (12)$$

with

$$I_\Lambda^{(0)}(m) = iN_c \int \frac{d^4p}{(2\pi)^4} \frac{\theta(\Lambda^2 - \vec{p}^2)}{p^2 - m^2 + i\epsilon}. \quad (13)$$

Its ‘‘empirical’’ value derived from QCD sum rules is

$$\langle\bar{\psi}_u\psi_u\rangle^{1/3} \simeq \langle\bar{\psi}_d\psi_d\rangle^{1/3} = -(240 \pm 20) \text{ MeV}. \quad (14)$$

- The current quark mass m_0 is fixed from the Gell-Mann, Oakes, Renner (GMOR) relation:

$$m_\pi^2 = \frac{-m_0 \langle\bar{\psi}\psi\rangle}{f_\pi^2}. \quad (15)$$

In the chiral limit, $m_0 = 0$ and $m_\pi = 0$.

The Goldberger-Treiman relation, which determines the pion-quark coupling g_π , follows from the previous relations:

$$m = g_\pi f_\pi \quad (16)$$

with $g_\pi^2 = (4I_\Lambda^{(1)}(m))^{-1}$.

We will first perform all our calculations with a finite value for the current quark mass m_0 , and then investigate the chiral limit, $m_0 \rightarrow 0$. The parameters obtained by imposing the constraints (11-15) are shown in Table 1.

4 Results at finite T and μ

We now extend the NJL model to finite temperature T and chemical potentials μ using the Matsubara formalism. We consider the isospin symmetric case, with an equal number (and therefore a single chemical potential) of u and d quarks. The quantity to be minimized at finite temperature is the thermodynamic potential:

$$\begin{aligned}\Omega(T, \mu) &= -T \sum_n \int \frac{d^3p}{(2\pi)^3} \frac{1}{2} \text{Tr} \ln \left(\frac{1}{T} \tilde{S}^{-1}(i\omega_n, \vec{p}) \right) \\ &+ \frac{\sigma^2}{2G} + \frac{|\Delta|^2}{2H},\end{aligned}\quad (17)$$

where $\omega_n = (2n + 1)\pi T$ are the Matsubara frequencies for fermions and the inverse quark propagator including the chemical potential μ is now defined as

$$\tilde{S}^{-1}(p^0, \vec{p}) = \begin{pmatrix} \not{p} - \hat{M} - \mu\gamma_0 & \Delta\gamma_5\tau_2 t_2 \\ -\Delta^* \gamma_5\tau_2 t_2 & \not{p} - \hat{M} + \mu\gamma_0 \end{pmatrix}.\quad (18)$$

Using the identity

$$\text{Tr} \ln(X) = \ln \det(X)\quad (19)$$

we can evaluate the trace in (17) and obtain

$$\frac{1}{2} \text{Tr} \ln \left(\frac{\tilde{S}^{-1}}{T}(i\omega_n, \vec{p}) \right) = 4 \ln \left(\frac{\omega_n^2 + (E^+)^2}{T^2} \right) + 4 \ln \left(\frac{\omega_n^2 + (E^-)^2}{T^2} \right),\quad (20)$$

where we have defined $E^\pm = \sqrt{(\epsilon^\pm)^2 + |\Delta|^2}$, with $\epsilon^\pm = \epsilon \pm \mu$, $\epsilon = \sqrt{\vec{p}^2 + m^2}$. Next we evaluate the Matsubara sum in eq. (17) using the following relation:

$$T \sum_{n=-\infty}^{\infty} \ln \left(\frac{\omega_n^2 + E^{\pm 2}}{T^2} \right) = E^\pm + 2T \ln(1 + \exp(-E^\pm/T)).\quad (21)$$

The thermodynamic potential becomes:

$$\begin{aligned}\Omega(T, \mu) &= -4 \int \frac{d^3p}{(2\pi)^3} \left[2T \ln \left(1 + \exp \left(-\frac{E^+}{T} \right) \right) + \right. \\ &+ \left. 2T \ln \left(1 + \exp \left(-\frac{E^-}{T} \right) \right) + (E^+ + E^-) \right] \theta(\Lambda^2 - \vec{p}^2) + \frac{\sigma^2}{2G} + \frac{|\Delta|^2}{2H}.\end{aligned}\quad (22)$$

In eqs. (20)-(22), the effective (constituent) quark mass m is related to the current quark mass and the σ field through eq. (10).

The mean values for the σ and Δ fields are determined by minimizing the thermodynamic potential. One obtains the following set of coupled equations that must be solved simultaneously in order to find the solutions for σ and $|\Delta|$:

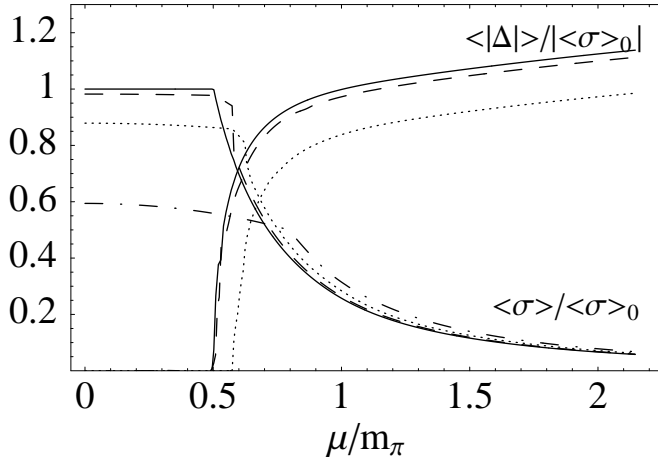


Figure 1: Scaled expectation values $\langle \sigma \rangle$ and $\langle |\Delta| \rangle$ as a function of the chemical potential for different temperatures. Continuous lines correspond to $T = 0$, dashed lines to $T = 100$ MeV, dotted lines to $T = 150$ MeV and the dashed-dotted line corresponds to $T = 200$ MeV ($\langle |\Delta| \rangle = 0$ in this case).

$$\begin{aligned}
 \sigma &= -\frac{2G}{\pi^2} \int dp p^2 \frac{m_0 - \sigma}{\epsilon} \left[\frac{\epsilon - \mu}{E^-} + \frac{\epsilon + \mu}{E^+} + \right. & (23) \\
 &\quad \left. - 2 \left(\frac{\epsilon - \mu}{(\exp(\frac{E^-}{T}) + 1) E^-} + \frac{\epsilon + \mu}{(\exp(\frac{E^+}{T}) + 1) E^+} \right) \right] \\
 |\Delta| &= \frac{2H}{\pi^2} \int dp p^2 \left[\frac{|\Delta|}{E^-} + \frac{|\Delta|}{E^+} - 2 \left(\frac{|\Delta|}{(\exp(\frac{E^-}{T}) + 1) E^-} + \frac{|\Delta|}{(\exp(\frac{E^+}{T}) + 1) E^+} \right) \right]
 \end{aligned}$$

In Fig. 1 we show our results for the scaled expectation values of the σ and Δ fields as a function of the chemical potential for different temperatures. One observes that at $T = 0$ the system undergoes a second order phase transition at a critical chemical potential $\mu_c = m_\pi/2$, as predicted by general arguments. The value of the pion mass that we consider here is the one evaluated in the model and shown in Table 1. So this model exhibits diquark condensation at chemical potentials larger than μ_c , where the value of the chiral condensate is correspondingly reduced. At $T = 0$, Δ is always non-vanishing for $\mu > \mu_c$: the diquark phase persists for large μ . For temperatures $T \gtrsim 200$ MeV, on the other hand, the diquark condensate vanishes even for large chemical potentials.

The chiral effective Lagrangian approach [11] predicts the following behaviour

for the diquark condensate as a function of the chemical potential at $\mu > \mu_c$:

$$\frac{\langle \psi\psi \rangle}{|\langle \bar{\psi}\psi \rangle_0|} = \frac{\langle |\Delta| \rangle}{|\langle \sigma \rangle_0|} = \sqrt{1 - \left(\frac{m_\pi}{2\mu}\right)^4}, \quad (24)$$

which means that $\langle |\Delta| \rangle$ should reach the vacuum expectation value of the (scaled) chiral condensate asymptotically as $\mu \rightarrow \infty$. In the NJL model, the scale of variation for $\mu > \mu_c$ is set by the momentum cutoff Λ . As a consequence, $|\Delta(\mu)|$ increases until $\mu \sim \Lambda$ (corresponding to $\mu/m_\pi \sim 5$). For larger values of μ the relevant interactions become weaker and $|\Delta|$ tends to decrease with μ . This feature is an artifact, however, since the applicability of the NJL model is limited to energy and momentum scales below Λ . For chemical potentials smaller than the cutoff scale the agreement between NJL and chiral Lagrangian calculations is excellent, as expected. At very large chemical potential, perturbative gluon exchange presumably takes over, with decreasing interaction strength as μ increases.

In Fig. 2 we show a comparison of our results for the scaled chiral and diquark condensates at $T = 0$ as a function of the chemical potential, with lattice data taken from ref. [27]. These data have been obtained by studying two-colour QCD with staggered fermions in the adjoint representation. It was found that the positive determinant sector behaves like a two-flavour theory. As we can see, the agreement of our results with lattice data is remarkable. The dashed lines are the predictions from chiral effective field theory.

In Fig. 3 we show the scaled $\langle \sigma \rangle$ and $\langle |\Delta| \rangle$ as a function of the temperature for different values of the chemical potential. In this way we find, as a function of the chemical potential, the critical temperature of the phase transition, so that we can draw the phase diagram of two-colour QCD as modelled in the NJL model. We show it in Fig. 4. At very small chemical potentials we have a transition from a system in which chiral symmetry is spontaneously broken to a system where it is restored (from region I to region II) with $\langle |\Delta| \rangle = 0$ in both phases. Region III is the superfluid phase with $\langle |\Delta| \rangle \neq 0$.

An interesting quantity is the baryonic density

$$\rho = -\frac{\partial \Omega(T, \mu)}{\partial \mu}. \quad (25)$$

The lattice data of ref. [27] show a scaled baryonic density defined as:

$$\tilde{\rho} = \frac{\rho}{4N_f f_\pi^2 m_\pi}. \quad (26)$$

Leading order chiral effective field theory [11] gives the following behaviour at $\mu > \mu_c$:

$$\tilde{\rho} = \frac{\mu}{2m_\pi} \left(1 - \left(\frac{m_\pi}{2\mu}\right)^4 \right). \quad (27)$$

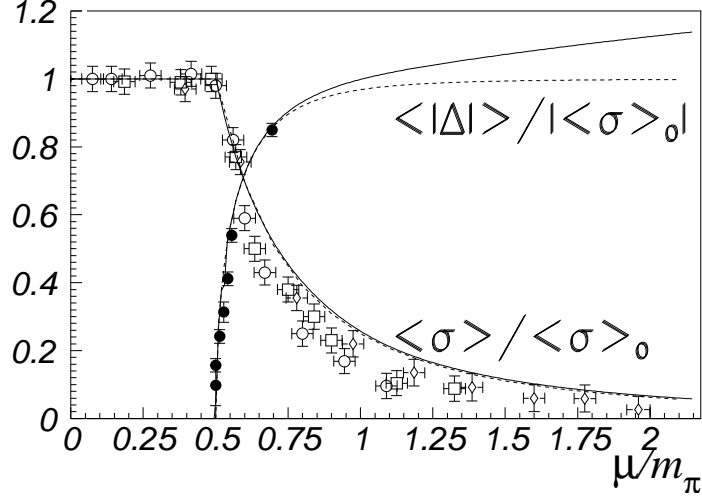


Figure 2: Scaled $\langle \sigma \rangle$ and $\langle |\Delta| \rangle$ as a function of the chemical potential at $T = 0$: our results (solid lines) are compared to the lattice data taken from ref. [27]. The different symbols (open circles, squares and diamonds) for the chiral condensate correspond to different values for the quark masses. The dashed lines are the predictions from chiral effective field theory [11].

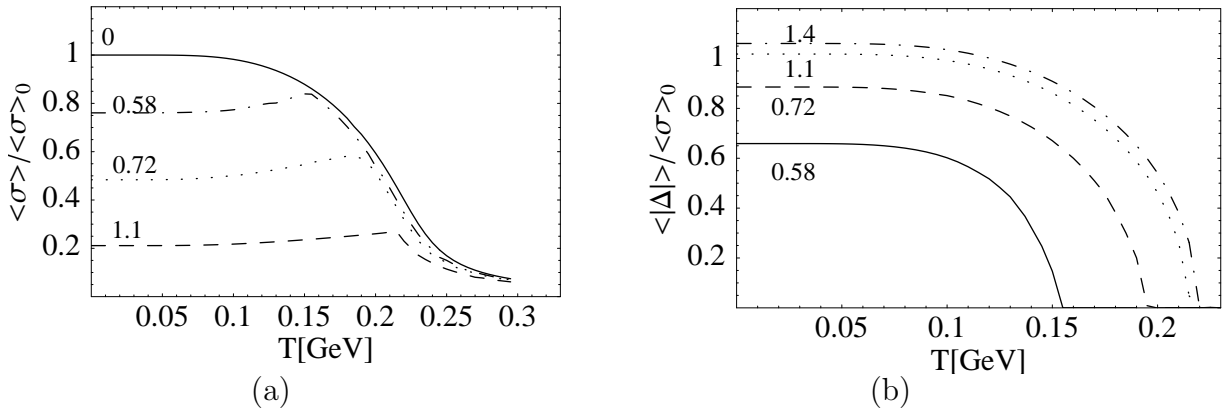


Figure 3: Scaled $\langle \sigma \rangle$ (a) and $\langle |\Delta| \rangle$ (b) as a function of temperature for different values of μ/m_π .

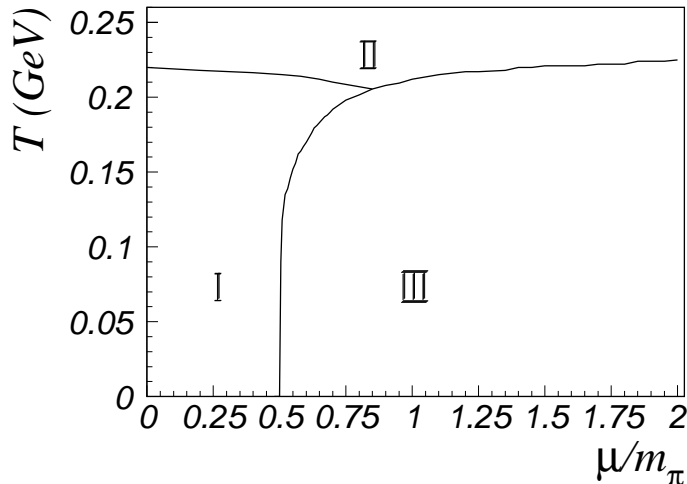


Figure 4: Phase diagram in the NJL model with two colours. The zone I is a region in which chiral symmetry is spontaneously broken, and $\langle |\Delta| \rangle = 0$; in region II chiral symmetry is restored, and again $\langle |\Delta| \rangle = 0$; region III is the superfluid phase in which $\langle |\Delta| \rangle \neq 0$.

Fig. 5 presents our results for the scaled baryonic density (26) as a function of the chemical potential at zero temperature, in comparison with the lattice data for the same quantity. Our results are in good agreement with lattice data at moderate chemical potentials, while for large chemical potentials the baryon density is underestimated. This difference may be caused by the mean-field approximation. Correlations between quasiparticles, not covered by this approximation, tend to become increasingly important with growing density.

4.1 Pion and scalar diquark properties

This Section presents our results for the masses of the (pseudo)-Goldstone bosons, namely the pion, the scalar diquark and the corresponding antidiquark.

In order to evaluate the masses of the bosonic fields, we expand the effective action

$$\mathcal{S}_{eff} = - \int d^4x \left[\frac{\sigma^2 + \vec{\pi}^2}{2G} + \frac{\Delta\Delta^*}{2H} \right] - \frac{i}{2} tr \int d^4x \ln (S^{-1}(x)). \quad (28)$$

in a power series of the meson and diquark fields around their mean field values. The second-order term of this expansion identifies the mass spectrum of mesons and diquarks. The resulting effective action in momentum space has the following form:

$$\mathcal{S}_{eff}^{(2)}(\sigma, \vec{\pi}, \Delta, \Delta^*) = -\frac{\sigma^2 + \vec{\pi}^2}{2G} - \frac{\Delta\Delta^*}{2H} + \frac{i}{4} tr \int \frac{d^4p}{(2\pi)^4} \left[\tilde{S}_0 A \tilde{S}_0 A \right] \quad (29)$$

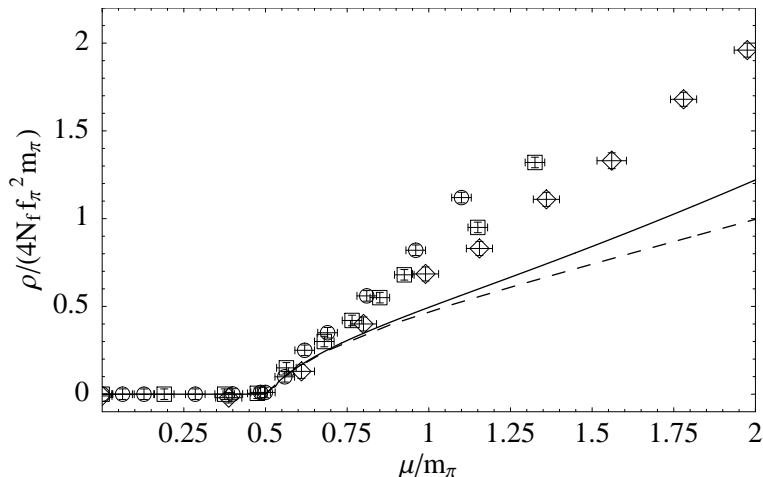


Figure 5: Scaled baryonic density as a function of the chemical potential at $T = 0$ (Continuous line). The lattice data are taken from ref. [27]. The different symbols correspond to different values for the quark masses. The dashed line is the prediction from chiral effective field theory [11].

where \tilde{S}_0 is the Nambu-Gorkov propagator (18) evaluated at the mean field values for the bosonic fields, and A is a matrix defined in the following way:

$$A = \begin{pmatrix} \sigma + i\gamma_5 \vec{\pi} \cdot \vec{\tau} & \Delta \gamma_5 \tau_2 t_2 \\ -\Delta^* \gamma_5 \tau_2 t_2 & \sigma - i\gamma_5 \vec{\pi} \cdot \vec{\tau} \end{pmatrix} \quad (30)$$

(see also [56]). By analyzing the second order action (29), one observes that mixing terms arise, at $\mu > \mu_c$, between the σ , Δ and Δ^* fields: these terms are proportional to $|\Delta|$, and the mixing occurs because the presence of a nonzero diquark condensate spontaneously breaks the baryon number symmetry. This feature was already found in [39]. The mass matrix turns out to have the following form:

$$M = \begin{pmatrix} \frac{\partial^2 \mathcal{S}_{eff}^{(2)}}{\partial \pi^2} & 0 & 0 & 0 \\ 0 & \frac{\partial^2 \mathcal{S}_{eff}^{(2)}}{\partial \sigma^2} & \frac{\partial^2 \mathcal{S}_{eff}^{(2)}}{\partial \sigma \partial \Delta} & \frac{\partial^2 \mathcal{S}_{eff}^{(2)}}{\partial \sigma \partial \Delta^*} \\ 0 & \frac{\partial^2 \mathcal{S}_{eff}^{(2)}}{\partial \Delta \partial \sigma} & \frac{\partial^2 \mathcal{S}_{eff}^{(2)}}{\partial \Delta^2} & \frac{\partial^2 \mathcal{S}_{eff}^{(2)}}{\partial \Delta \partial \Delta^*} \\ 0 & \frac{\partial^2 \mathcal{S}_{eff}^{(2)}}{\partial \Delta^* \partial \sigma} & \frac{\partial^2 \mathcal{S}_{eff}^{(2)}}{\partial \Delta^* \partial \Delta} & \frac{\partial^2 \mathcal{S}_{eff}^{(2)}}{\partial \Delta^*{}^2} \end{pmatrix}, \quad (31)$$

and the masses of the various modes are found by solving the equation

$$\det(M) = 0. \quad (32)$$

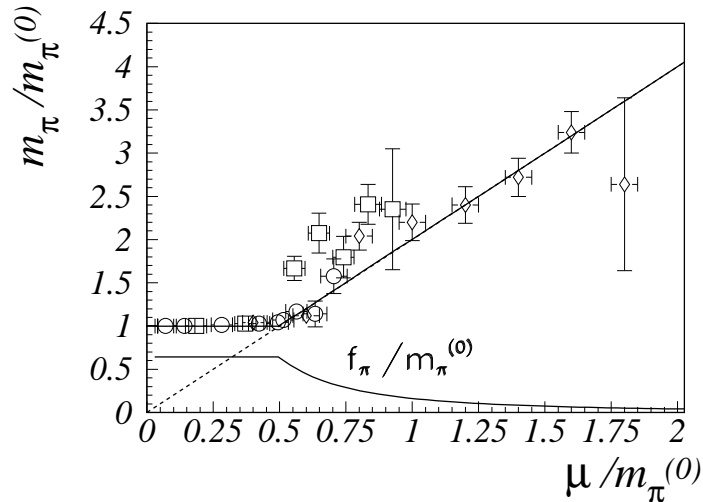


Figure 6: Scaled pion mass as a function of $\mu/m_\pi^{(0)}$ at $T = 0$ (continuous line). The lattice data are taken from ref. [27] and have been rescaled in order to show dimensionless quantities. The different symbols correspond to different values for the quark masses. The dashed line is $m_\pi = 2\mu$, as predicted in leading-order chiral effective field theory [11]. Also shown is the (scaled) pion decay constant $f_\pi/m_\pi^{(0)}$ and its evolution with increasing μ .

Evidently the pion fields do not mix with the others, while the σ , the diquark and the antidiquark fields mix in the phase with $|\Delta| \neq 0$.

The behaviour of the scaled pion mass as a function of the chemical potential is shown in Fig. 6, in comparison to the lattice data. The pion mass increases linearly with the chemical potential at $\mu > \mu_c$. This behaviour was anticipated in the calculations by Kogut *et al.* [11]. They in fact predicted for m_π the following behaviour at $\mu > \mu_c$:

$$m_\pi = 2\mu, \quad (33)$$

as indicated by the dashed line in Fig. 6. Our result is in very good agreement with both the lattice data and the predictions using the leading-order chiral effective Lagrangian.

The behaviour of the pion and σ masses and of the pion decay constant as functions of temperature at $\mu = 0$ is shown in Fig. 7. At temperatures T exceeding the critical T_c for the chiral transition at which $\langle \sigma \rangle$ tends to zero, m_σ becomes equal to the pion mass and both masses rise continuously with increasing T . The pion decay constant tends to zero at the same time.

Next, consider the other two bosonic modes of the theory: the scalar diquark and its antidiquark. The behaviour of their masses at finite chemical potential is shown in Fig. 8 in comparison to the pion mass: at $\mu = 0$ they are all degenerate, as predicted on the basis of general arguments, but they behave in different ways as

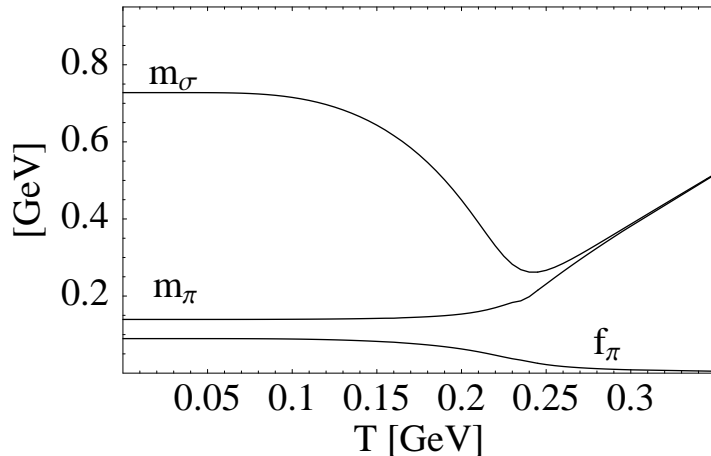


Figure 7: Pion mass, σ boson mass and pion decay constant as a function of temperature at $\mu = 0$.

the chemical potential increases: for $\mu < \mu_c = m_\pi^{(0)}/2$ the pion, which does not carry baryon charge, is not affected by μ , while the diquark and antidiquark masses are shifted according to their baryon number $B = \pm 1$. They follow in fact the behaviour observed also in chiral effective field theory [11]:

$$m_\Delta = m_\pi - 2\mu, \quad m_{\Delta^*} = m_\pi + 2\mu. \quad (34)$$

For $\mu > \mu_c$, the appearance of the diquark condensate spontaneously breaks the baryon number symmetry. The scalar modes (diquark, antidiquark and sigma) get mixed. The new eigenmodes are linear combinations of the original quasiparticle states. By solving eq. (32) we find the masses of the new orthogonal modes. One of them, which we denote by $\tilde{\Delta}$, is massless and can be identified with the true Goldstone boson of the theory, corresponding to the spontaneous breaking of the baryon number ($U(1)$) symmetry. The other two modes are massive. One of them, which we denote by $\tilde{\Delta}^*$, follows the behaviour derived in the paper by Kogut *et al.*:

$$M_{\tilde{\Delta}^*} = 2\mu\sqrt{1 + 3(m_\pi/2\mu)^4}. \quad (35)$$

5 Chiral limit

In the chiral limit $m_0 \rightarrow 0$ ($m_\pi \rightarrow 0$), and at $\mu = 0$, the thermodynamic potential (22) (with $G = H$) is a function only of $\sigma^2 + |\Delta|^2$, as already mentioned. This is a natural outcome once the relation between the coefficients G and H is fixed through the Fierz transformation of the colour current-current interaction (see eq. (4)). As

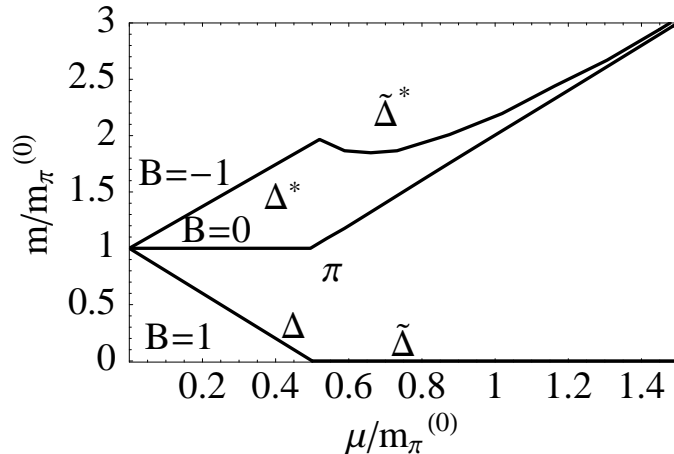


Figure 8: Spectrum of pions and diquarks/antidiquarks as a function of the (scaled) chemical potential at zero temperature.

a result, Ω is invariant under the rotation which connects the chiral and the diquark condensate along the circle $\sigma^2 + |\Delta|^2 = \text{const}$. Because of this symmetry, the chiral condensate is indistinguishable from the diquark condensate for $m_0 = \mu = 0$, so that a state with finite $\langle \sigma \rangle$ can always be transformed into a state with finite $\langle |\Delta| \rangle$ and $\langle \sigma \rangle = 0$. The phases with spontaneously broken chiral and baryon number symmetries are degenerate in this limit.

As soon as the chemical potential takes a finite value, the favourable phase is the one with a non-zero diquark condensate and zero chiral condensate. This is evident from Fig. 9 which shows the contour plots of the thermodynamic potential as a function of σ and $|\Delta|$. In the left panel we have $T = \mu = 0$ and the rotational invariance is evident. In the right panel we have introduced a very small chemical potential, which is nevertheless sufficient to break the rotational invariance along $R^2 = \langle \sigma \rangle^2 + \langle |\Delta| \rangle^2$ and favour the phase in which $\langle \sigma \rangle = 0$ and $\langle |\Delta| \rangle \neq 0$.

Minimizing the thermodynamic potential of the system, one finds the mean-field values of the chiral and diquark condensates. Our results in Fig. 10 display $\langle |\Delta| \rangle$ as a function of temperature for different chemical potentials. The chiral condensate is always equal to zero in those cases.

In Fig. 11 the phase diagram of the two-colour NJL model in the chiral limit is compared to the one using a finite value of the bare quark mass m_0 . As one can see, the phase boundaries for $m_0 = 0$ and $m_0 \neq 0$ become identical at large chemical potentials, whereas at small μ they show a qualitatively different behaviour. In the exact chiral limit there are only two phases in the theory: the superfluid phase with $\langle |\Delta| \rangle \neq 0$ and the high-temperature phase with $\langle |\Delta| \rangle = 0$, separated by a critical temperature of about 0.2 GeV.

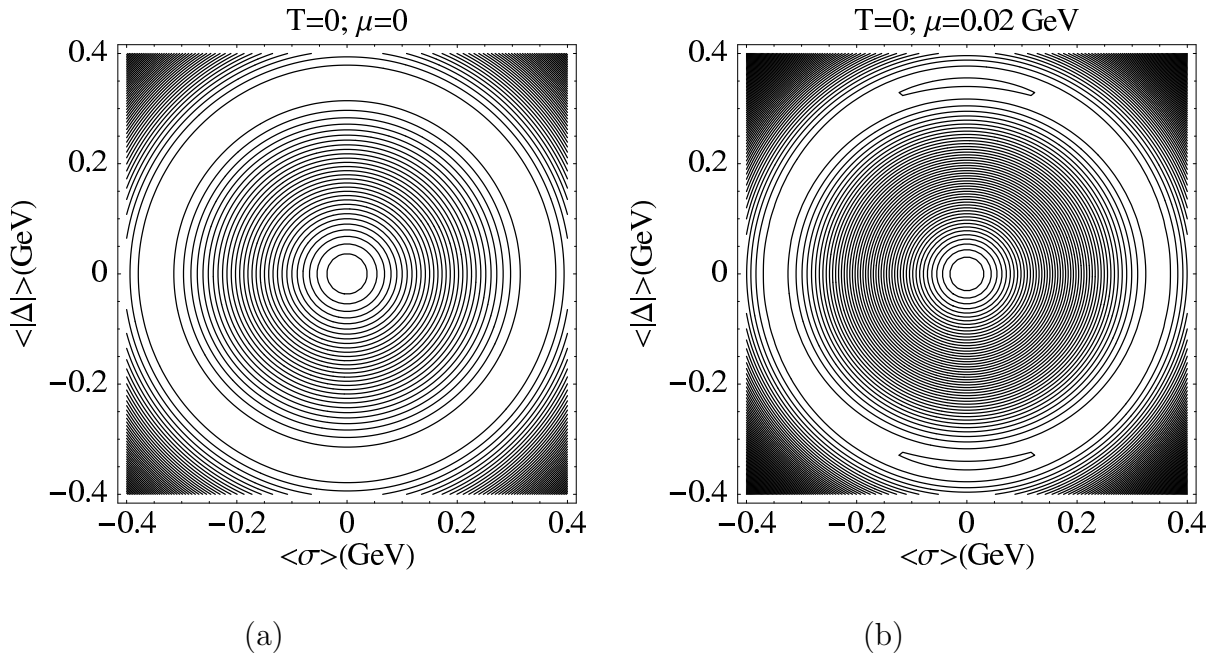


Figure 9: Contour plots of the thermodynamic potential in the chiral limit ($m_0 = 0$) as a function of σ and Δ for $T = \mu = 0$ (a) and $T = 0$ and $\mu = 20$ MeV (b).

Consider next the pion and diquark masses in the chiral limit and their variations with increasing chemical potential. The chiral condensate is always equal to zero in this limit. Consequently, the $\tilde{\Delta}$ mode is a true Goldstone boson and its mass is always equal to zero, while the $\tilde{\Delta}^*$ and pion masses are degenerate. Explicit symmetry breaking by a finite chemical potential lets these masses scale as $m_{\tilde{\Delta}^*} = m_{\pi} = 2\mu$. The degeneracy of $\tilde{\Delta}^*$ and π is removed as soon as a small non-zero quark mass m_0 is introduced. This also gives a finite mass to the $\tilde{\Delta}$ mode, which is again equal to zero above $\mu_c = m_{\pi^{(0)}}/2$.

Fig. 12 illustrates this situation for a very small value of m_0 (~ 0.1 MeV). The critical value μ_c of the chemical potential is identified as $\mu_c = m_{\pi}^{(0)}/2$, as discussed previously, but now of course with a very small value of the vacuum pion mass $m_{\pi}^{(0)}$. As the limit $m_0 \rightarrow 0$ is approached, $m_{\pi}^{(0)} \rightarrow 0$ and $\mu_c \rightarrow 0$: the low-temperature system is always in the superfluid phase for any value of μ . At $\mu = 0$ we recover the exact Pauli-Gürsey symmetry, with vanishing pion and diquark masses.

6 Conclusions

We have investigated a two-colour and two-flavour Nambu and Jona-Lasinio model at finite temperature and finite baryon chemical potential, with the primary aim

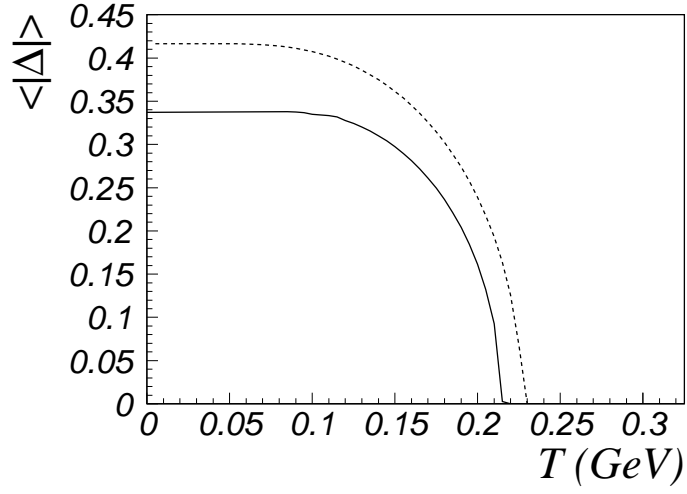


Figure 10: Mean field value of the $|\Delta|$ field as a function of temperature for $\mu = 0$ (continuous) and $\mu = 350$ MeV (dashed).

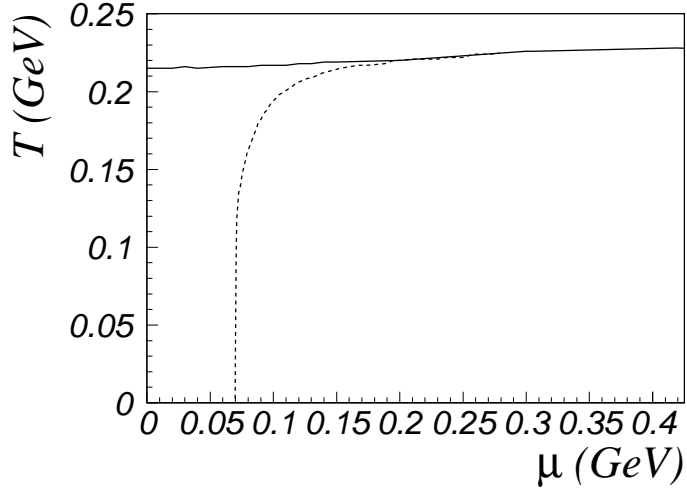


Figure 11: Comparison between the phase diagram of two-colour QCD in the chiral limit (continuous) and for bare quark mass $m_0 \neq 0$ (dashed).

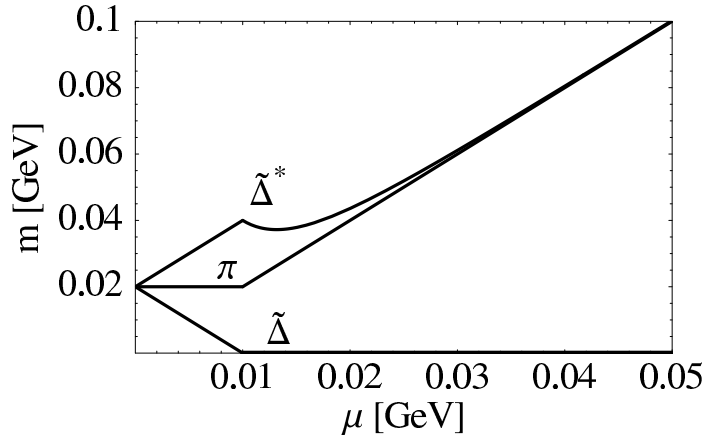


Figure 12: Pion and diquark/antidiquark masses approaching the chiral limit ($m_0 \simeq 0.1$ MeV). In the exact chiral limit, $m_{\tilde{\Delta}^*} = m_\pi = 2\mu$ and $m_{\tilde{\Delta}} \equiv 0$.

of exploring the capability of such a model to reproduce the thermodynamics of $N_c = 2$ lattice QCD. The starting point is the assumption that gluon dynamics can be integrated out and reduced to a local interaction between quark colour currents. By Fierz rearrangement, this implies a one-to-one correspondence between interactions in colour singlet quark-antiquark and diquark channels (the Pauli-Gürsey symmetry).

The resulting spontaneous (dynamical) symmetry breaking pattern identifies pseudoscalar Goldstone bosons (pions) and scalar diquarks as the thermodynamically active quasiparticles. The successful comparison with $N_c = 2$ lattice data indicates that this simple NJL model does indeed draw a remarkably realistic picture of the quasiparticle dynamics emerging from $N_c = 2$ QCD, even though the original local colour gauge symmetry of QCD has been reduced to a global colour $SU(2)$ symmetry in the NJL quasi-particle model. We note that colour (triplet) quark-antiquark modes which are the remnants of gluon degrees of freedom in this model, are far removed from the low-energy spectrum. Poles of the respective Bethe-Salpeter amplitudes appear at mass scales several times the NJL cutoff scale [57].

We confirm that a diquark condensate develops at chemical potentials $\mu > \mu_c = m_\pi/2$. The correlated evolution of the chiral and diquark condensates with increasing μ , as observed in $N_c = 2$ lattice QCD, is very well reproduced. Had we started from NJL four-point interactions with independent, arbitrary coupling strengths in quark-antiquark and diquark channels, the condensate pattern would have been quite different. It appears that modelling the low-energy dynamics of $N_c = 2$ QCD is already done surprisingly well when using just a colour current-current interaction with a single strength parameter.

The calculated baryon density, obtained by taking the derivative of the thermo-

dynamic potential with respect to the chemical potential, describes the corresponding lattice results well in the range $\mu < 2\mu_c$. Deviations occur at larger μ which presumably indicate the increasing importance of correlations between quasiparticles beyond the mean-field approximation.

The NJL model also permits an instructive study of the way in which this system behaves in the chiral limit which is not directly accessible in lattice computations. In particular, the limits of vanishing quark mass and vanishing baryon chemical potential do not commute, as expected, and have to be handled with care.

The low-energy physics of QCD differs qualitatively between $N_c = 2$ and $N_c = 3$ because of the very different nature of the baryonic quasiparticles in these two theories. Nevertheless, the success of the present studies encourages further extended investigations also for $N_c = 3$ thermodynamics, using NJL type quasiparticle approaches above the critical temperature for deconfinement, in close contact with lattice QCD simulations.

We thank Pietro Faccioli, Jiri Hosek, Georges Ripka and Michael Thaler for stimulating discussions and valuable comments.

Appendix

We start from the colour current interaction (1) and show that performing a Fierz transformation we obtain the Lagrangian (2) with the coupling coefficients related by (4).

In order to demonstrate this identity for the coefficient of the scalar diquark interaction (H) we must Fierz transform this interaction into the qq channel, while for G we must Fierz transform into the $\bar{q}q$ channel.

Let us start with H ; we rewrite the interaction term of eq. (1) and keep track explicitly of all colour, flavour and Dirac indices:

$$\begin{aligned} \mathcal{L}_{int}^c &= -G_c \sum_{a=1}^3 (\bar{\psi} \gamma^a t^a \psi)^2 \\ &= -G_c \sum_{a=1}^3 \left[\bar{\psi}_{i,p,\mu} \psi_{j,q,\nu} \bar{\psi}_{k,r,\rho} \psi_{l,s,\sigma} (\gamma^a)_{\mu\nu} (\gamma^a)_{\rho\sigma} (t_a)_{ij} (t_a)_{kl} \delta_{pq} \delta_{rs} \right] \end{aligned} \quad (36)$$

with:

i, j, k, l	\rightarrow	colour indices
p, q, r, s	\rightarrow	flavour indices
μ, ν, ρ, σ	\rightarrow	Dirac indices.

We start by performing the Fierz transformation for the flavour indices using the following relation

$$\delta_{pq}\delta_{rs} = \frac{1}{2} \sum_{b=0}^3 (\tau_b)_{pr} (\tau_b)_{sq}, \quad (37)$$

where we have defined

$$\tau_0 = \begin{pmatrix} 1 & 0 \\ 0 & 1 \end{pmatrix} \quad \text{and} \quad \tau_b = \text{Pauli matrices with } b = 1, 2, 3, \quad (38)$$

thus obtaining

$$\mathcal{L}_{int}^c == -\frac{1}{2} G_c \sum_{a=1}^3 \sum_{b=0}^3 \left[\bar{\psi}_{i,p,\mu} \psi_{j,q,\nu} \bar{\psi}_{k,r,\rho} \psi_{l,s,\sigma} (\gamma_\alpha)_{\mu\nu} (\gamma^\alpha)_{\rho\sigma} (t_a)_{ij} (t_a)_{kl} (\tau_b)_{pr} (\tau_b)_{sq} \right] \quad (39)$$

In order to Fierz-transform the colour indices we use the relation

$$\sum_{a=1}^3 (t_a)_{ij} (t_a)_{kl} = \frac{1}{2} \left[\delta_{ik} \delta_{lj} + (t_1)_{ik} (t_1)_{lj} + (t_3)_{ik} (t_3)_{lj} \right] - \frac{3}{2} (t_2)_{ik} (t_2)_{lj}, \quad (40)$$

thus obtaining

$$\begin{aligned} \mathcal{L}_{int}^c &= -\frac{1}{4} G_c \sum_{b=0}^3 \left[\bar{\psi}_{i,p,\mu} \psi_{j,q,\nu} \bar{\psi}_{k,r,\rho} \psi_{l,s,\sigma} (\gamma_\alpha)_{\mu\nu} (\gamma^\alpha)_{\rho\sigma} [\delta_{ik} \delta_{lj} + \right. \\ &\quad \left. + (t_1)_{ik} (t_1)_{lj} + (t_3)_{ik} (t_3)_{lj} - 3 (t_2)_{ik} (t_2)_{lj} \right] (\tau_b)_{pr} (\tau_b)_{sq}. \end{aligned} \quad (41)$$

At the end we perform the Fierz transformation for the Dirac indices and find

$$\begin{aligned} \mathcal{L}_{int}^c &= -\frac{1}{4} G_c \sum_{b=0}^3 \left[\bar{\psi}_{i,p,\mu} \psi_{j,q,\nu} \bar{\psi}_{k,r,\rho} \psi_{l,s,\sigma} \left((C^*)_{\mu\rho} (C)_{\sigma\nu} - \frac{1}{2} (\gamma_\alpha C^*)_{\mu\rho} (C \gamma^\alpha)_{\sigma\nu} + \right. \right. \\ &\quad \left. \left. - \frac{1}{2} (\gamma_\alpha \gamma_5 C^*)_{\mu\rho} (C \gamma^\alpha \gamma_5)_{\sigma\nu} + (i \gamma_5 C^*)_{\mu\rho} (i C \gamma_5)_{\sigma\nu} \right) (\delta_{ik} \delta_{lj} + \right. \\ &\quad \left. + (t_1)_{ik} (t_1)_{lj} + (t_3)_{ik} (t_3)_{lj} - 3 (t_2)_{ik} (t_2)_{lj} \right) (\tau_b)_{pr} (\tau_b)_{sq} \Big] = \\ &= -\frac{1}{4} G_c \sum_{b=0}^3 \sum_{S=0,1,3} \left[(\bar{\psi} \tau_b t_S C \bar{\psi}^T) (\psi^T C \tau_b t_S \psi) + (i \bar{\psi} \gamma_5 \tau_b t_S C \bar{\psi}^T) (i \psi^T C \gamma_5 \tau_b t_S \psi) \right. \\ &\quad \left. - \frac{1}{2} (\bar{\psi} \gamma_\alpha \tau_b t_S C \bar{\psi}^T) (\psi^T C \gamma_\alpha \tau_b t_S \psi) - \frac{1}{2} (\bar{\psi} \gamma_\alpha \gamma_5 \tau_b t_S C \bar{\psi}^T) (\psi^T C \gamma_\alpha \gamma_5 \tau_b t_S \psi) \right] \\ &\quad + \frac{3}{4} G_c \sum_{b=0}^3 \left[(\bar{\psi} \tau_b t_2 C \bar{\psi}^T) (\psi^T C \tau_b t_2 \psi) + (i \bar{\psi} \gamma_5 \tau_b t_2 C \bar{\psi}^T) (i \psi^T C \gamma_5 \tau_b t_2 \psi) \right. \\ &\quad \left. - \frac{1}{2} (\bar{\psi} \gamma_\alpha \tau_b t_2 C \bar{\psi}^T) (\psi^T C \gamma_\alpha \tau_b t_2 \psi) - \frac{1}{2} (\bar{\psi} \gamma_\alpha \gamma_5 \tau_b t_2 C \bar{\psi}^T) (\psi^T C \gamma_\alpha \gamma_5 \tau_b t_2 \psi) \right] \quad (42) \end{aligned}$$

where we have introduced the charge conjugation matrix operator for fermions $C = i\gamma_0\gamma_2$. We can easily read from eq. (42) the coefficient of the scalar diquark channel:

$$H = \frac{3}{2}G_c. \quad (43)$$

Next we show that also $G = 3G_c/2$, starting from eq. (36) and performing a Fierz transformation into the $\bar{q}q$ channel.

We start from the flavour- $SU(2)$ identity

$$\delta_{pq}\delta_{rs} = \frac{1}{2} \sum_{b=0}^3 (\tau_b)_{ps} (\tau_b)_{rq} \quad (44)$$

and obtain

$$\mathcal{L}_{int}^c = -\frac{1}{2}G_c \sum_{a=1}^3 \sum_{b=0}^3 \left[\bar{\psi}_{i,p,\mu} \psi_{j,q,\nu} \bar{\psi}_{k,r,\rho} \psi_{l,s,\sigma} (\gamma_\alpha)_{\mu\nu} (\gamma^\alpha)_{\rho\sigma} (t_a)_{ij} (t_a)_{kl} (\tau_b)_{ps} (\tau_b)_{rq} \right]. \quad (45)$$

Then we transform colour indices by using

$$\sum_{a=1}^3 (t_a)_{ij} (t_a)_{kl} = \frac{3}{2} \delta_{il} \delta_{kj} - \frac{1}{2} \sum_{c=1}^3 (t_c)_{il} (t_c)_{kj} \quad (46)$$

and find

$$\begin{aligned} \mathcal{L}_{int}^c &= -\frac{1}{4}G_c \sum_{b=0}^3 \left[\bar{\psi}_{i,p,\mu} \psi_{j,q,\nu} \bar{\psi}_{k,r,\rho} \psi_{l,s,\sigma} (\gamma_\alpha)_{\mu\nu} (\gamma^\alpha)_{\rho\sigma} (3\delta_{il}\delta_{kj} \right. \\ &\quad \left. - \sum_{c=1}^3 (t_c)_{il} (t_c)_{kj}) (\tau_b)_{ps} (\tau_b)_{rq} \right]. \end{aligned} \quad (47)$$

Finally the Dirac Fierz transformation leads to:

$$\begin{aligned} \mathcal{L}_{int}^c &= -\frac{1}{4}G_c \sum_{b=0}^3 \left[\bar{\psi}_{i,p,\mu} \psi_{j,q,\nu} \bar{\psi}_{k,r,\rho} \psi_{l,s,\sigma} \left(\delta_{\mu\sigma} \delta_{\rho\nu} - \frac{1}{2} (\gamma_\alpha)_{\mu\sigma} (\gamma^\alpha)_{\rho\nu} - \frac{1}{2} (\gamma_\alpha \gamma_5)_{\mu\sigma} (\gamma^\alpha \gamma_5)_{\rho\nu} + \right. \right. \\ &\quad \left. \left. (i\gamma_5)_{\mu\sigma} (i\gamma_5)_{\rho\nu} \right) \left(3\delta_{il}\delta_{kj} - \sum_{c=1}^3 (t_c)_{il} (t_c)_{kj} \right) (\tau_b)_{ps} (\tau_b)_{rq} \right] = \\ &= \frac{1}{4}G_c \sum_{b=0}^3 \left\{ 3 \left[(\bar{\psi}\tau_b\psi)^2 + (i\bar{\psi}\gamma_5\tau_b\psi)^2 - \frac{1}{2} (\bar{\psi}\gamma_\alpha\tau_b\psi)^2 - \frac{1}{2} (\bar{\psi}\gamma_\alpha\gamma_5\tau_b\psi)^2 \right] \right. \\ &\quad \left. - \sum_{a=1}^3 \left[(\bar{\psi}t_a\tau_b\psi)^2 + (i\bar{\psi}\gamma_5t_a\tau_b\psi)^2 - \frac{1}{2} (\bar{\psi}\gamma_\mu t_a\tau_b\psi)^2 - \frac{1}{2} (\bar{\psi}\gamma_\mu\gamma_5t_a\tau_b\psi)^2 \right] \right\} \end{aligned}$$

from which we can easily read

$$G = \frac{3}{2}G_c. \quad (48)$$

References

- [1] F. Karsch, Lecture Notes in Physics (Springer) **583**, 209 (2002).
- [2] S. Muroya, A. Nakamura, C. Nonaka, and T. Takaishi, Prog. Theor. Phys. **110**, 615 (2003).
- [3] F. Karsch, K. Redlich, and A. Tawfik, Phys. Lett. **B571**, 67 (2003).
- [4] Z. Fodor and S. D. Katz, JHEP **0203**, 014 (2002).
- [5] B. C. Barrois, Nucl. Phys. **B129**, 390 (1977).
- [6] D. Bailin and A. Love, Phys. Reports **107**, 325 (1984).
- [7] M. Iwasaki and T. Iwado, Phys. Lett. **B350**, 163 (1995).
- [8] M. G. Alford, K. Rajagopal, and F. Wilczek, Phys. Lett. **B422**, 247 (1998).
- [9] K. Rajagopal, Nucl. Phys. **A661**, 150 (1999).
- [10] R. Rapp, T. Schaefer, E. V. Shuryak, and M. Velkovsky, Phys. Rev. Lett. **81**, 53 (1998).
- [11] J. B. Kogut, M. A. Stephanov, D. Toublan, J. J. M. Verbaarschot, and A. Zhitnitsky, Nucl. Phys. **B582**, 477 (2000).
- [12] M. A. Halasz, A. D. Jackson, R. E. Shrock, M. A. Stephanov, and J. J. M. Verbaarschot, Phys. Rev. **D58**, 096007 (1998).
- [13] E. Dagotto, F. Karsch, and A. Moreo, Phys. Lett. **B169**, 421 (1986).
- [14] E. Dagotto, A. Moreo, and U. Wolff, Phys. Lett. **B186**, 395 (1987).
- [15] J. B. Kogut, M. A. Stephanov, and D. Toublan, Phys. Lett. **B464**, 183 (1999).
- [16] K. Splittorff, D. T. Son, and M. A. Stephanov, Phys. Rev. **D64**, 016003 (2001).
- [17] K. Splittorff, D. Toublan, and J. J. M. Verbaarschot, Nucl. Phys. **B620**, 290 (2002).
- [18] K. Splittorff, D. Toublan, and J. J. M. Verbaarschot, Nucl. Phys. **B639**, 524 (2002).
- [19] B. Vanderheyden and A. D. Jackson, Phys. Rev. **D64**, 074016 (2001).
- [20] B. Klein, D. Toublan, and J. J. M. Verbaarschot, (2004), hep-ph/0405180.

- [21] J. Wirstam, J. T. Lenaghan, and K. Splittorff, Phys. Rev. **D67**, 034021 (2003).
- [22] M.-P. Lombardo, (1999), hep-lat/9907025.
- [23] M. P. Lombardo, M. L. Paciello, S. Petrarca, and B. Taglienti, Nucl. Phys. Proc. Suppl. **129**, 635 (2004).
- [24] S. Hands, J. B. Kogut, M.-P. Lombardo, and S. E. Morrison, Nucl. Phys. **B558**, 327 (1999).
- [25] S. Hands *et al.*, Eur. Phys. J. **C17**, 285 (2000).
- [26] S. J. Hands, B. Kogut, S. E. Morrison, and D. K. Sinclair, Nucl. Phys. Proc. Suppl. **94**, 457 (2001).
- [27] S. Hands, I. Montvay, L. Scorzato, and J. Skullerud, Eur. Phys. J. **C22**, 451 (2001).
- [28] R. Aloisio, A. Galante, V. Azcoiti, G. Di Carlo, and A. F. Grillo, Guangzhou 2000, Non-perturbative methods and lattice QCD , 123 (2000).
- [29] R. Aloisio, V. Azcoiti, G. Di Carlo, A. Galante, and A. F. Grillo, Phys. Lett. **B493**, 189 (2000).
- [30] R. Aloisio, V. Azcoiti, G. Di Carlo, A. Galante, and A. F. Grillo, Nucl. Phys. **B606**, 322 (2001).
- [31] Y. Liu, O. Miyamura, A. Nakamura, and T. Takaishi, Guangzhou 2000, Non-perturbative methods and lattice QCD , 132 (2000).
- [32] S. Muroya, A. Nakamura, and C. Nonaka, Nucl. Phys. Proc. Suppl. **94**, 469 (2001).
- [33] S. Muroya, A. Nakamura, and C. Nonaka, Phys. Lett. **B551**, 305 (2003).
- [34] B. Alles, M. D’Elia, M. P. Lombardo, and M. Pepe, Nucl. Phys. Proc. Suppl. **94**, 441 (2001).
- [35] B. Alles, M. D’Elia, M.-P. Lombardo, and M. Pepe, (2002), hep-lat/0210039.
- [36] E. Bittner, M.-P. Lombardo, H. Markum, and R. Pullirsch, Nucl. Phys. Proc. Suppl. **94**, 445 (2001).
- [37] J. B. Kogut, D. Toublan, and D. K. Sinclair, Phys. Lett. **B514**, 77 (2001).
- [38] J. B. Kogut, D. K. Sinclair, S. J. Hands, and S. E. Morrison, Phys. Rev. **D64**, 094505 (2001).

- [39] J. B. Kogut, D. Toublan, and D. K. Sinclair, Phys. Rev. **D68**, 054507 (2003).
- [40] J. B. Kogut, D. Toublan, and D. K. Sinclair, Nucl. Phys. **B642**, 181 (2002).
- [41] J.-I. Skullerud, S. Ejiri, S. Hands, and L. Scorzato, (2003), hep-lat/0312002.
- [42] Y. Nambu and G. Jona-Lasinio, Phys. Rev. **122**, 345 (1961).
- [43] Y. Nambu and G. Jona-Lasinio, Phys. Rev. **124**, 246 (1961).
- [44] U. Vogl and W. Weise, Prog. Part. Nucl. Phys. **27**, 195 (1991).
- [45] S. P. Klevansky, Rev. Mod. Phys. **64**, 649 (1992).
- [46] T. Hatsuda and T. Kunihiro, Phys. Reports **247**, 221 (1994).
- [47] J. Berges and K. Rajagopal, Nucl. Phys. **B538**, 215 (1999).
- [48] K. Langfeld and M. Rho, Nucl. Phys. **A660**, 475 (1999).
- [49] M. Buballa, J. Hosek, and M. Oertel, Phys. Rev. **D65**, 014018 (2002).
- [50] M. Buballa, J. Hosek, and M. Oertel, Phys. Rev. Lett. **90**, 182002 (2003).
- [51] D. Blaschke, M. K. Volkov, and V. L. Yudichev, Eur. Phys. J. **A17**, 103 (2003).
- [52] R. Nebauer and J. Aichelin, Phys. Rev. **C65**, 045204 (2002).
- [53] M. Buballa and M. Oertel, Nucl. Phys. **A703**, 770 (2002).
- [54] F. Neumann, M. Buballa, and M. Oertel, Nucl. Phys. **A714**, 481 (2003).
- [55] M. Buballa, (2004), hep-ph/0402234, Submitted to Phys. Reports.
- [56] D. Blaschke, D. Ebert, K. G. Klimenko, M. K. Volkov, and V. L. Yudichev, (2004), hep-ph/0403151.
- [57] M. Thaler, private communication .